

Spatial Entropy-based Cost Function for Gray and Color Image Segmentation with Dynamic Optimal Partitioning

MK Quweider

CIS Department, University of Texas, Brownsville Brownsville, Texas 78520, USA

Summary

In this paper, we present a novel thresholding-based segmentation algorithm that combines entropy, image spatial information, and dynamic programming to non-uniformly quantize an image in a more efficient and effective way for subsequent processing. Combined with information related to the structural content present in the image (activity/busyness of pixels with respect to their immediate neighbors), an entropy-based cost function is derived and used with the one-dimensional histogram probability distribution function of the image. The image quantization/ segmentation algorithm uses dynamic programming based on a recently introduced algorithm for optimal partitioning on an interval, and allow the selection of a broad range gray level to be present in the output image; binarization of an image is accomplished by having only two gray levels in the output image. Applications of the algorithm to quantization of gray-level as well as color images in the RGB and HSV color spaces are presented. Image simulations give very good results compared to many existing methods, while maintaining low computational complexity in terms of storage and processing requirements.

Keywords

Entropy, Spatial information, Dynamic programming, Cost functions, Optimal partitioning on an interval, Image segmentation.

1. Introduction

Quantization is an essential part in any digital imaging acquisition system. As a formed analog/continuous image is sampled on a grid of given resolution—spatial resolution that determines the width and height—the intensity values at the grid locations must be digitized to produce amplitudes of a given resolution. In most image acquisition modalities, the resolution used, given as bits per pixel (bpp), is 8 bits-per-pixel corresponding to 256 gray levels. More generally, k -bits per pixel give rise to 2^k unique levels, with higher values of k being typical in medical diagnostics and industrial inspection systems. Color images are characterized by three separate channel (components) corresponding to a given color-space model such as the additive RGB (red, green, and blue) model which is prevalent in most acquisition hardware devices and the display industry devices (projectors, screens, televisions, etc.) or the subtractive YMC (yellow, cyan, and magenta) model, which is prevalent in the printing

industry. The HSV (hues, saturation, and value) color space model is used in applications based on perceptual properties of the human visual system.

It is rare for an image processing system to work directly on the acquired image without first representing it in a more compact, economical, and efficient form (from a processing point of view), while keeping the structural and informational content intact. The step is done mainly for efficiency purposes. One way of achieving this is to reduce the number of gray levels present in the image (for gray-level images) or one or more of its components (for color images). Reducing the number of gray levels in an image is a fundamental issue in many image processing and computer vision applications including segmentation, thresholding, lossy compression, and image retrieval, just to name few. Segmentation is closely related to the gray level reduction problem. Although there exists many methods for segmentation, thresholding remains one of the most attractive and simple ones. Quantization can be seen as a multi-level thresholding problem, which is the view we adopt in this paper; when one-threshold is generated (two quantization levels) for the output image, the problem reduces to that of binarization, and when multiple thresholds are generated, the output image quantized gray levels can be judiciously selected between the thresholds to produce a pleasing and ready-to-process image.

This paper presents a new multi-level thresholding method for image segmentation that allows the user to reduce the number of gray levels, in a hierarchical fashion, from the original number present in the image all the way down to two gray levels, corresponding to a binary version of the image. Our contribution to the problem is twofold: first, we present an entropy-based dynamic cost function that automatically adapts to the size of the region under examination so far; second, we integrate the cost function seamlessly with an interval optimal partitioning algorithm that uses dynamic programming. In section 2 and 3, we review thresholding an entropy-based thresholding respectively. In section 4 we briefly describe optimal partitioning; section 5 presents the entropy-based segmentation algorithm in details. Section 6 presents simulations with comparative results of some existing methods. Conclusions and future work are given in section 7.

2. Thresholding

The goal of image segmentation is to extract meaningful objects, or regions, from an input image. Thresholding is a simple and effective way to segment an image, especially those that have a bi-modal histogram probability density function. The popularity of thresholding stems from its intuitive interpretation, simplicity, and ease of computation. The technique has found many applications in object recognition, automatic inspection, robotics, machine vision, document and text analysis, medical image analysis, remote sensing, surveillance, and computer graphics, among many others [1-27].

Given a digital image $I(i,j)$, of dimension N_x by N_y , with $I(i,j)$ representing the intensity at location (i,j) , $1 \leq i \leq N_x$, $1 \leq j \leq N_y$, $0 \leq I(i,j) \leq L-1$, a two-level quantized output image (using single threshold) is given by:

$$Q_2(i, j) = \begin{cases} q_0 & 0 \leq I(i,j) < T_0 \\ q_1 & T_0 \leq I(i,j) < L-1 \end{cases} \quad (1)$$

Here, L represents the maximum number of gray levels ($L=2^k$, with k termed the pixel-depth or the number of bits/pixel for the image). For a multi-level thresholded image, the quantized output image is given by

$$Q_M(i, j) = \begin{cases} q_0 & 0 \leq I(i,j) < T_0 \\ q_1 & T_0 \leq I(i,j) < T_1 \\ \dots & \dots \\ q_{M-1} & T_{M-2} \leq I(i,j) < L-1 \end{cases} \quad (2)$$

Early methods of thresholding have used the image histogram (or its normalized version) to calculate the thresholds, while later methods have incorporate pixel dependencies and spatial and structural information into the thresholds computation. A plethora of methods have been reported in the literature over the past fifty years; see for example [31] for many insightful reviews on most thresholding techniques based on image histograms, iterative refinement, objective optimization, region properties, and variants of entropy measures. Among these methods, entropy-based thresholding are based on information theory concepts, and they have played an important role among the other techniques. Many reported methods try to incorporate spatial and structural information [1-27] using the image histogram, image co-occurrence matrix, or an optimized objective function [1][6][7]. Examples include optimizing second-order entropy extracted from the image co-occurrence matrix; optimizing relative or cross entropy [11-15]; or optimizing excess entropy of the image [32].

All the subsequent tasks to thresholding, including feature extraction, object recognition, and classification, rely heavily on the quality of the image segmentation process. Enhancing segmentation by incorporating spatial information into the selection of thresholds to quantize the image is both desirable and challenging. Section 3 addresses exactly this issue.

3. Entropy-based Thresholding

Entropy is a measure of information content that has its origins in the seminal work of C. Shannon on coding and information theory [10]. Given a discrete source of data, S ,

$$S = \{s_0, s_1, s_2, \dots, s_{n-2}, s_{n-1}\},$$

With an associated probability distribution function:

$$P(S) = \{p(s_0), p(s_1), p(s_2), \dots, p(s_{n-2}), p(s_{n-1})\}$$

such that $\sum_{i=0}^{n-1} p(s_i) = 1$,

Shannon defined the entropy of the source S as

$$H(S) = \sum_{i=0}^{i=n-1} -p(s_i) \log_2(p(s_i)), \quad (3)$$

For an image, entropy is a quantity used to describe the amount of uncertainty or lack of structure. When pixels are considered alone, entropy can be calculated using the normalized histogram of the image—its probability distribution function—using:

$$Entropy = E(f(x, y)) = \sum_{l=0}^{L=2^k-1} -p_l \log_2(p_l). \quad (4)$$

As a robust information-theoretic approach, entropy is used in many segmentation and quantization techniques. These techniques include finding optimal thresholds by maximizing Shannon's entropy, or minimizing relative entropy, also known as Kullback-Leibler information distance. An excellent survey on the many variants of entropy and relative entropy is given by Chang and others in [31]. Many researchers seek to improve entropy by using the image spatial information to produce a more visually-based measure. Most spatially-oriented entropy measures work with two-dimensional histograms or the gray-level co-occurrence matrix to capture transitions between gray levels. Other techniques include local entropy and joint entropy, which can be seen as extensions of the maximum entropy method of Pun and Kapur [18]. Recently, excess entropy, which measures the structural information of the image, has been applied successfully to segment images [32].

In this paper, we redefine the histogram-based entropy to incorporate spatial information about the image in the

form of busyness that reflects the activity of each gray level. To do this, we use the following measure for entropy

$$SpatialEntropy = SE(H) = \sum_{l=0}^{L-1} -p_l \log(p_l / m_l), \tag{5}$$

where m_l is a busyness or activity weighting factor. The inclusion of this factor makes thresholding less dependent on the size of objects or background present in the image. Several approaches can be used to define this factor; in this paper, we define m_l in three different but closely related ways. The three measures use a local neighborhood as shown in figure 1. The first method measures the variance; the second method measures the local gradient; the third methods measure local spatial variation relating to its texture patterns. Due to space limitation, we report results on the first method of variance-based busyness since the other methods gave virtually similar results as will be reported in future publications.

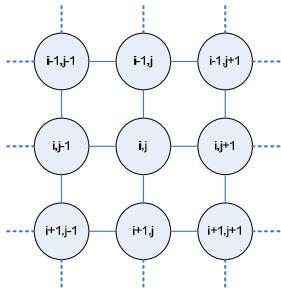


Fig. 1 NxN neighborhood definition for variance and gradient

3.1 Variance-based Busyness Measure

Referring to figure 1, the variance-based busyness measure, m_l , is defined as the average of all variances of all $N \times N$ neighborhood of a pixel whose intensity level has the values of l .

$$m_l = \frac{1}{|I(i,j) \in l|} \sum_{i=1}^{N_x} \sum_{j=1}^{N_y} \sigma_{l,i,j}^2, l = 0,1,2,\dots, L-1 \tag{6}$$

$$\sigma_{l,i,j}^2 = \begin{cases} \sigma_{NxN}^2(i,j) & \text{if } I(i,j) = l \\ 0 & \text{if } I(i,j) \neq l \end{cases} \tag{7}$$

The $N \times N$ neighborhood of a pixel at spatial location (i,j) is defined as shown in figure 1 (for the case of $N=3$). To produce the m_l values, we scan the image, in a pre-processing stage, and compute the variance value $\sigma_{NxN}^2(i,j)$, at each (i,j) .

$$\sigma_{NxN}^2(i,j) = \left\{ \frac{1}{|NxN|} \sum_{(i,j) \in NxN} (I(i,j) - \mu_{NxN})^2 \right.$$

$$\mu_{NxN} = \left\{ \frac{1}{|NxN|} \sum_{(i,j) \in NxN} (I(i,j)) \right. \tag{8}$$

The spatial entropy measure described above is adapted from A.D. Brink [13], who defined a similar measure on a pixel-by-pixel level, considering the whole image as a huge set of elements, with the gray level of each pixel as the count of the number of photons that reaches that given pixel. The total number of photons in the image, G , is therefore computed by summing all the gray levels in the image as follows:

$$G = \sum_{l=0}^{L-1} g_l \tag{9}$$

We redefined the measure to work for the histogram since our algorithm works with optimal partitioning on an interval (as described in the next section) to produce any number of quantization levels, the above definition keeps the computational complexity to a minimum, especially since the optimal partitioning algorithm has $O(L^2)$ complexity, which would be prohibitive for the whole image.

3.2 Gradient-based Busyness Measure

For the gradient-based busyness measure, referring to figure 1, the measure, m_l , is defined as the combined magnitude of the horizontal and the vertical gradient in the $N \times N$ as given by:

$$m_l = \frac{1}{|I(i,j) \in l|} \sum_{i=1}^{N_x} \sum_{j=1}^{N_y} M_l(i,j), l = 0,1,2,\dots, L-1, \text{ where}$$

$$M(i,j) = \sqrt{g_x^2 + g_y^2} \tag{10}$$

Where $M(i,j)$ is the gradient image, formed from the magnitude of the gradient vector $(g_x, g_y)^t$ at each location (i,j) . For g_x , and g_y , we have used the Sobel operators, defined using the masks shown in figure 2.

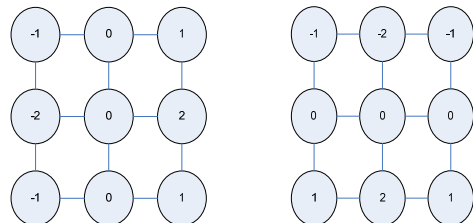


Fig. 2 Mask operators used for the gradient-based busyness measure definition

3.3 Texture-based Busyness Measure

For the texture-based busyness measure, referring to figure 3, the measure, m_i , is defined as the local binary pattern of the 8 neighbors of the center pixel. The binary pattern is created by using the intensity, gray level value, of the center pixel as a threshold in comparison with these eight neighbors. When thresholded, the 8 neighbors, numbered 0-7, will give rise to a binary number $b_0b_1b_2b_3b_4b_5b_6b_7$ which is then used as the m_i measure. LBP are known to be effective in capturing local structure characteristics and can be made invariant to specific transformation such as rotation.

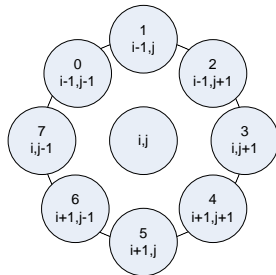


Fig. 3 Local binary pattern used for the texture-based busyness measure definition

4. Optimal Partitioning on an Interval

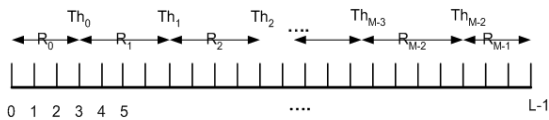


Fig. 4 Histogram Partitioning into M Regions Using M-1 Thresholds

The goal of thresholding is to partition the histogram of the image in an optimal way with respect to some predefined objective function or region properties. If R represents the histogram, our goal, then, is to partition this histogram into M mutually exclusive regions (partition elements or blocks), which mathematically can be written as

$$\{R_i | i = 0, 1, 2, \dots, M - 1\} \text{ such that } \bigcup_{i=0}^{M-1} R_i = R \text{ and } R_i \cap R_j = \emptyset \text{ for } i \neq j.$$

Figure 4 shows the desired partitioning. By defining a partition element as a set of one or more contiguous cells from the histogram, and defining an appropriate cost function, an optimal partitioning can be reached where the number of thresholds automatically determines the number of segmented or quantized regions (partition elements) in the image. All pixels between two successive thresholds within the histogram belong to the same region. A cost function, $C(R_i)$, is associated with the i^{th} region or partition element with the overall cost over the histogram R , denoted as $C(R)$, being the sum of the costs of the

elements of the partition. This can be expressed as follows:

$$C(R) = \sum_{i=0}^{M-1} C(R_i), \tag{11}$$

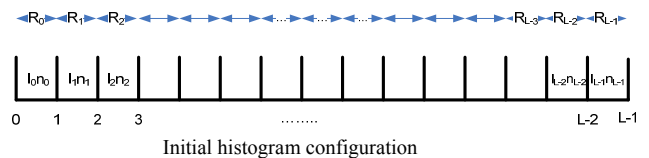
Jackson, Scargle and others [28-30], have recently developed a dynamic programming technique that solves this problem in $O(L^2)$ where L is the length of the signal (histogram) to be partitioned. A cost function is associated with each possible partition. The algorithm searches the exponentially large space of partitions of L data points in time $O(L^2)$. As discussed in [28], the algorithm is guaranteed to find the exact global optimum, automatically determines the model order (the number of thresholds), and has a convenient real-time mode. Additionally, the algorithm has a Prior parameter that can be set base on our desired level of segmentation, with higher values giving coarse segmentation, less number of regions, and smaller values giving fine segmentation, or larger number of segments. The algorithm can be summarized as follows.

1. Decide the prior parameter and the form of the cost function
2. Set $optimal(-1) = 0$; set $n = 0$
3. Given $optimal(j)$ for $j = 0, 1, \dots, n$
 - a. Compute $optimal(n+1)$ as given in [28], for $j = 0, 1, \dots, n+1$
 - b. Store the value of j where the maximum occurred in $lastChange(n+1)$
 - c. Set $n = n+1$
 - d. If $n = L$, stop
4. Extract the set of $M-1$ thresholds as:

$$Th = \begin{cases} Th_{M-2} = lastChange(L-1) \\ Th_{M-3} = lastChange(Th_{M-2}-1) \\ Th_i = lastChange(Th_{i+1}-1) \\ \dots \\ Th_0 = lastChange(Th_1) \end{cases} \tag{12}$$

As we can see from the third step, the thresholds are traced backward in reverse order and then used to partition the histogram accordingly.

A. Entropy-based Cost Function



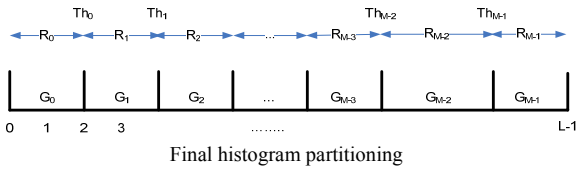


Fig. 5 Histogram initialization for the entropy-based cost function

Essential to the success of the optimal partitioning algorithm is the choice of a suitable cost function. In [30], we have introduced some cost functions (some of which were adopted from [28-29]) based either on Normal distribution or Bayesian posterior for a segmented Poisson model. The cost function we adopted is based on an entropy measure that is weighted with additional information related the spatial structures of the image. Given our histogram, R , the cost function C is defined as

$$C(R) = \sum_{i=0}^{M-1} E(R_i), \text{ with}$$

$$E(R_i) = - \sum_{g_i \in R_i} \frac{g_i}{G_i} \log \left(\frac{g_i / G_i}{m_i} \right) \quad (13)$$

$$g_i = n_i \cdot l_i, \text{ and } G_i = \sum_{i \in R_i} g_i$$

One important observation for our thresholding problem is the fact that the cost function has the desired property that it depends on only two quantities: the sum of all the gray levels g_i present in an interval, R_i , and the number of cells in that interval, which are called *sufficient statistics*. The cost model is basically identifying regions, by their homogeneity as defined by the maximum entropy in that region. The prior relates to the probability distribution of the number of partition elements, or segments. This parameter can be taken or interpreted to represent prior knowledge about the complexity of the image as represented by its histogram and whether it has many objects or segments. Its value is somewhat context-dependent and can be determined with simulations, re-sampling in the bootstrap sense, or with other numerical studies. We can also look at the prior as a tweaking parameter to reduce or increase the number of final partition elements (objects) in the image. It acts something like a smoothness parameter with large values giving smaller number of partition elements; nevertheless, it does not implement smoothing in the sense of smearing of the levels of the image. The optimal partitioning works with any additive cost function [13], which makes it applicable to a wide range of applications. It is worthy to note that a transformation can always be applied to convert a multiplicative cost function into an additive one.

5. Algorithmic Details

The flow chart of the algorithm is given in Fig. 1, illustrated with the Lena image. At the heart of the algorithm are the entropy-based function and the OP algorithms that is driven by it. Based on the histogram model, dynamic partitioning of an interval, and the choice of a cost function, we introduce the generalized gray level reduction algorithm. The algorithm within its main framework and with only a different prior input (treated as an adjustable parameter) can produce any desired number of thresholds or gray levels. The algorithm has a limit-up approach where we start with all the present gray levels in the image as regions. The algorithm then reduces the number of gray levels by selecting a subset of them (thresholds) as boundaries or significant change points.

Following are the general steps for the algorithm:

1. Create the modified histogram as described in sections 3,4
2. Decide on a prior value based on complexity of the histogram structure and the final number of regions desired in the image
3. The optimal partitioning algorithm receives the histogram as an interval with the cost function and the prior. Its outputs is the set of thresholds, $\{Th_i \mid i = 0, 1, 2, \dots, M - 2\}$, defining each region R_i .
4. Create the quantized values $\{q_i \mid i = 0, 1, 2, \dots, M - 1\}$ based on the thresholds found in the previous step

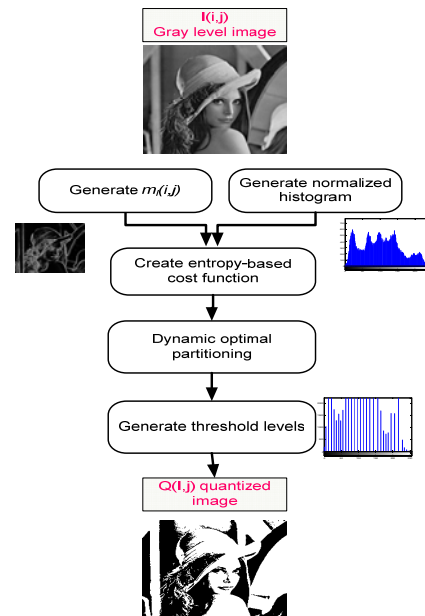


Fig. 6 Flow diagram of the entropy-based cost function thresholding algorithm

We used the set of thresholds in the above algorithm to create a new set of reduced quantized levels in the image. Each quantized value q_i was calculated from two successive thresholds Th_{i-1} and Th_i . A weighted average of the gray levels between the two thresholds is then chosen to represent the region R_i with all the gray levels that lie in that region. The Mathematical details were given in [30]. In addition to the image and its dimensions, the algorithm takes one parameter and a choice of a cost function. The parameter describes the prior for the number of change points, which is sometimes called a hyper-parameter. It implicitly determines the number of classes, with large values giving smaller number of gray levels in the output image. The cost function can be modified to fit the application at hand. In addition to the Poisson cost function used in this paper, other cost functions based on Gaussian distribution [28] or entropy [11-14] can be used as well. Some of these cost functions have the advantage of incorporating local features from the image, albeit in a different way that our method and at higher computational cost.

6. Experimental Results

We present typical quantization and thresholding results using the Entropy-based Dynamic Optimal Partitioning algorithm developed in section 5. Results are presented for gray-level and for color images in both the RGB space as well as the HSV space. We use the Lena image to present the gray-level results and the color Lena, Baboon, and F-16 for the color results. The images are of different content type with respect to their histogram distribution. The histograms range from relatively bimodal to multi-peaked. Additionally, the images are different in terms of their content ranging from low to high detail. These images are 256x256 in size with 8 bit pixel-depth giving rise to a maximum of 256 gray levels.

a. Quantization of Gray-Level Images

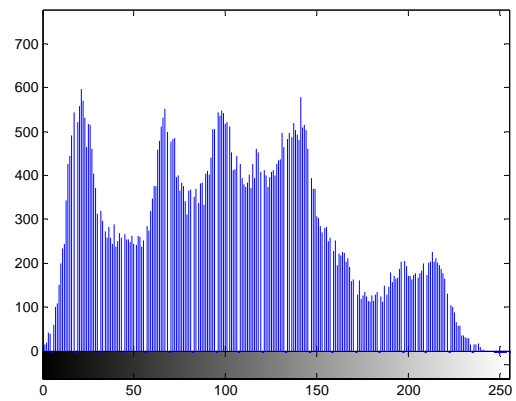


Fig. 7 Original Lena image (gray-level) and its histogram

For gray-level images we have only one input channel or plane, known as the luminance Y-channel. The histogram and the variance image are created in the pre-processing stage and are then used as inputs for the spatial entropy-based cost function. Optimal partitioning is run, using the formulated cost function and a prior value (to be discussed in detail in this section), to produce the set of thresholds. The thresholds, in turn, are used to create the quantize image, $Q(i,j)$. Each quantized value q_i is calculated based on the two successive thresholds Th_{i-1} and Th_i it lies within (with 0 being the first threshold and L-1 as the last one). A weighted average of the gray levels between the two thresholds is then chosen to represent the image region of all pixels whose value lies between the two thresholds. The parameter describes the prior for the number of change points, which is sometimes called a hyper-parameter. It implicitly determines the number of classes, with large values giving smaller number of gray levels in the output image. We can look at the results as representing three types of problems: Gray level reduction, multi-level thresholding (segmentation), and single-level thresholding (binarization). All three problems are actually the same from the point of view of our algorithm. Depending on the number of desired regions and the ultimate application for the output image, a single threshold, few thresholds (usually less than 10), or many thresholds are produced at a time. The prior provided to the algorithm is adjusted to give the desired number of thresholds. Table 1 gives the number of gray levels present in the original Lena image, presented in figure 7. Table 2 and 3 give the NCP prior values used to create the indicated number of gray-levels or color levels (in the case of color thresholding), and Fig. 8 shows the results of running our algorithm on the Lena image producing 2, 4, 8, 16, 32, and 64 quantization levels. The number of gray levels produced was decided by the prior on the number of regions present in the histogram. Figures 8, 9, and 10 show binarized Lena images with other existing methods such as Papamarkos Neural thresholding and K-means. On the other hand, Figure 11 compares our algorithm with

the Otsu, Kittler and Illingworth, Reddi et al, Kapur et al., and Papamarkos et al methods for the special case of two gray levels. Images in the figures show the comparability of our algorithm at the smaller number of shareholding levels, and its superiority at the higher number of thresholding levels. Comparing the results for higher number of gray levels is practically impossible as some of the algorithms are not applicable or not available. We can see that our algorithm gives very pleasing results compared to the indicated methods. It captures more local details especially in busy areas that are characterized by the presence of edges, transitions, or textures. Essentially, we see that our algorithm does a good job in areas of high activity or details. This is expected since our entropy is weighted by a measure related to the level of activity around a specific gray level.

6.1 Quantization of noisy gray-level images

The algorithm also shows robustness under mild noise levels as figure 11 demonstrates, where we have included the binarized image for zero mean Gaussian noise with different variance levels. The noisy images and their thresholded binary counterparts are shown in the figure. We have tried noise levels of standard deviation of 10, 20, and 50, corresponding to small, mild, and severe noise levels. With the values of 10, and 20, we are able to reproduce an object almost identical to the no-noise case; however, as the noise level dominates the image, as in the case of standard deviation of 50, it becomes harder to separate the object from the background, even though it is still visually distinct. The thresholded images were post processed with a 3x3 smoothing Gaussian windows. The post processing ads a pleasing blurring effect to the image and gets rid of isolated impulsive noise points.

b. Quantization of Color Images

To work with color images, we extend the results of the gray-level images by working on the components of the color image separately. We present the results for two common color spaces: the RGB and the HSV.

6.1.1 RGB color space

The RGB space is the most frequently used color space in image processing. Since color cameras, scanners and displays are most often provided with direct RGB signal input or output. The high similarity and correlation of the R, G, and B components, especially for natural scenes, motivated us to use the gray-level or intensity algorithm uniformly to all three planes; we also know that when mostly $R \sim G \sim B$, the resultant image has mainly shades of gray. The NCP prior used was almost the same for all the three images (definitely, the same order of magnitude). Figure 13 shows the quantized results for the Lena,

Baboon, and F-16 images with the indicated number of quantization levels; as we mentioned, Each R, G, and B image has the indicated number of quantization level. Table 2 presents the NCP prior used to produce each image. The 3-tuple value is that R, G, and B planes respectively. Close inspection of the images show that they preserve their overall structure and color content at all levels, with blocking effect starting to show with 16 levels or below. Close inspection of the images show preservation of details in the busy areas in the Lena, Baboon, and F-16 images.

6.1.2 HSV color space

The second color space we used in our study is the HSV. In this model, hue represents the impression related to the dominant wavelength of the color stimulus. The saturation corresponds to relative color purity (lack of white in the color) and in case of a pure color it is equal to 100%. Colors with zero saturation are grey levels. Maximum intensity is sensed as pure white, minimum intensity as pure black. Figure 14 shows the quantized image for the Lena, Baboon, and F-16 images. The results are robust and resemble those obtained for the gray level cases and those of the RGB color model.

TABLE 1
ORIGINAL NUMBER OF GRAY LEVELS PRESENT IN EACH IMAGE

Image	No.
Lena	230

TABLE 2
NCP PRIOR VALUES FOR THE RGB COLOR CASE

NCP Prior			
No. Q-Levels	Lena	Baboon	F-16
8	[5.50;5.55;5.50]	[6.60;6.72;6.60]	[5.83;5.99;6.30]
16	[4.75;4.90;4.75]	[5.90;5.99;5.95]	[5.25;5.30;5.65]
32	[4.05;4.25;4.15]	[5.19;5.30;5.25]	[4.52;4.60;5.00]
64	[3.302;3.53;3.4]	[4.47;4.59;4.5]	[3.87;3.95;4.37]
128	[2.55;2.80;2.63]	[3.63;3.83;3.84]	[3.08;3.17;3.10]

TABLE 3
NCP PRIOR VALUES FOR THE HSV COLOR CASE

NCP Prior			
No. Q-Levels	Lena	Baboon	F-16
8	5.500	6.700	5.600
16	4.700	6.040	4.800
32	4.050	5.310	4.120
64	3.290	4.570	3.390
128	3.535	3.739	2.690

Conclusion

In this paper we presented new algorithm for image thresholding, segmentation and quantization based on a spatially-weighted entropy function of the image histogram and optimal partitioning on an interval using dynamic programming. The algorithm was presented for gray level as well as color images in the RGB and the HSV color-space domains. The algorithm works in a fine-to-coarse way, allowing the user to specify the number of gray levels to be present in the output image. This number can range from the original number of levels present in the image all the way down to two levels, (which corresponds to creating a binary output image). The optimal partitioning algorithm has a moderate computational efficiency of $O(L^2)$ proportional to the square of the number of unique gray levels present in the image. Its memory requirement grows only linearly with L . The algorithm can be easily incorporated with other algorithms such as region growing, edge detection and lossy compression. Future work will tackle some of the remaining issues including the speed of the algorithm and the quantification of the prior parameter to achieve a predetermined number of thresholds in a more systematic way; we are interested in direct higher-dimensional application of the entropy cost function optimal partitioning. Incorporating texture based features is of great interest, especially in image segmentation and region-based image retrieval systems.

Acknowledgment

Initial work on applications of OP in image processing was conducted at NASA-Ames Research Center under the supervision of Dr. Jeffery D. Scargle. His guidance and hospitality during my stay are greatly appreciated.

References

- [1]. A.S. Abutaleb, "Automatic thresholding of gray-level pictures using two-dimensional entropy," *Computer Vision, Graphics, and Image Processing*, vol. 47, pp. 22–32, 1989.
- [2]. T. Peli, and D. Malah, "A Study of edge detection algorithms," *Computer Graphics and Image Processing*, vol. 20, pp.1-2, 1982.
- [3]. P. K. Sahoo, S. Soltani, and A. K. C. Wong, "A survey of thresholding techniques," *Comput. Vis. Graph. Image Process.*, vol. 41, pp. 233–260, 1988.
- [4]. N. R. Pal and S. K. Pal, "A review on image segmentation techniques," *Pattern Recognit.*, vol. 26, pp. 1277–1294, Sep. 1993.
- [5]. M. Sezgin and B. Sankur, "Survey over image thresholding techniques and quantitative performance evaluation," *J. Electron. Imaging*, vol. 13, pp. 146–168, 2004.
- [6]. N. Otsu, "A threshold selection method from gray-level histograms," *IEEE Trans. Syst., Man, Cybern.*, vol. 9, pp. 62–66, 1979.
- [7]. J. Kittler, and J. Illingworth, "Minimum error thresholding," *Pattern Recognition*, vol. 19, pp. 41-47, 1986.
- [8]. N. R. Pal and S. K. Pal, "Entropic thresholding," *Signal Process.*, vol. 16, pp. 97–108, Feb. 1989.
- [9]. J. Kittler and J. Illingworth, "On threshold selection using clustering criteria," *IEEE Trans. Syst., Man, Cybern.*, vol.15, pp. 652–655, 1985.
- [10]. C. E. Shannon, "A mathematical theory of communication," *Bell Syst. Tech. J.*, vol. 27, pp. 379–423, 1948
- [11]. A. Brink, "Thresholding of digital images using two-dimensional entropies," *Pattern Recognition*, vol. 25, pp. 803-808, 1992.
- [12]. A. Brink, "Gray-level thresholding of images using a correlation criterion," *Pattern Recognition Letters*, vol. 9, pp. 335-341, 1989.
- [13]. A. Brink, "Minimum spatial entropy threshold selection," *IEE Proc.-Vis. Image Signal Process.*, vol. 142(3), pp. 128-132, 1995.
- [14]. A. Brink, "Using spatial information as an aid to maximum entropy image threshold selection," *Pattern Recognition Letters*, vol. 17(1), pp. 29-36, 1996.
- [15]. L. Cao, Z. Shi, and E. Cheng, "Fast automatic multilevel thresholding," *Electronic Letters*, vol. 38, pp. 868-870, 2002.
- [16]. C. Chang, C. Chang, and S. Hwang, "A Connectionist approach for thresholding," *Proc. Int'l Conf. Pattern Recognition*, vol. 11, pp. 522-525, 1992.
- [17]. J. Kapur, P. Sahoo, and A. Wong, "A new method for gray-level picture thresholding using the entropy of the histogram," *Computer Vision, Graphics and Image Processing*, vol. 29, pp. 273–285, 1985.
- [18]. T. Pun, "A new method for gray-level picture Thresholding using the entropy of the histogram," *Signal Processing*, vol. 2, pp. 223–237, 1980.
- [19]. S. Lee, S. Chung, and R. Park, "A comparative performance study of several global thresholding techniques for segmentation," *Computer Vision, Graphics and Image Processing*, vol. 52, pp. 171-190, 1990.
- [20]. K. Chung, and W. Chen, "Fast adaptive PNN-based thresholding algorithms," *Pattern Recognition*, vol. 36, pp. 2793-2804, 2003.
- [21]. Y. Chang, A. Fu, H. Yan, and M. Zhao, "Efficient two-level image thresholding method based on Bayesian formulation and the maximum entropy principle," *Optical Engineering*, vol. 41, pp. 2487-2498, 2002.
- [22]. N. Pal, and S. Pal, "Object-background segmentation using new definitions of entropy," *IEE Proceedings- Computers and Digital Techniques*. Vol. 136, pp. 284-295, 1989.
- [23]. S. Reddi, S. Rudin, and H. Keshavan, "An optimal multiple threshold scheme for image segmentation," *IEEE Trans. Syst., Man, Cybern.*, vol.14, pp. 661–665, 1984.
- [24]. N. Papamarkos, and A. and Atsalakis, "Gray-level reduction using local spatial Features," *Computer Vision and Image Understanding*, vol. 78, pp. 336-350, 2000.
- [25]. N. Papamarkos, and B. Gatos, "A New approach for multi-threshold selection," *Computer Vision, Graphics, and Image Processing*, vol. 56, pp.357-370, 1994.

- [26]. L. Lam , S. Lee, and C. Suen, "Thinning methodologies - a comprehensive survey," *IEEE Trans. PAMI*, vol. 14, pp. 869-885, 1992.
- [27]. O. Trier, and T. Taxt, "Evaluation of binarization methods for document images," *IEEE Trans. PAMI*, vol. 17, pp. 312-315, 1995.
- [28]. B. Jackson, J. Scargle, et. al. "An algorithm for optimal partitioning of data on an interval," *IEEE Signal Processing Letters*, vol. 12, pp. 105-108, 2005.
- [29]. J. Scargle and M.K. Quweider, "Edge Detection Using Dynamic Optimal Partitioning," *IEEE ICASSP-2006*, vol. 2, pp. 705-708, 2006.
- [30]. M.K. Quweider, J.D. Scargle and B. Jackson, "Grey level reduction for segmentation, thresholding and binarisation of images based on optimal partitioning on an interval," *IET Image Process*, vol. 1, pp. 103-111, 2007.
- [31]. C. Chang, Y. Du, J. Wang, S. Guo, and P. Thouin, "Survey and comparative analysis of entropy and relative entropy thresholding techniques," *IEE Proc. Vision, Image and Signal*, vol. 153, pp. 837-850, 2006.
- [32]. A. Bardera, I. Boada1, M. Feixas, and M. Sbert, "Image Segmentation Using Excess Entropy," *Signal Processing Systems*, vol. 54, pp. 205-214, 2009.



M K Quweider is an Associate Professor of Computer & Information Sciences at the U. of Texas at Brownsville. He received his Ph.D. in Engineering Science (Multimedia and Imaging Specialty) and B.S. in Electrical Engineering, M.S. in Applied Mathematics, M.S. in Engineering Science, and M.S. in Biomedical Engineering all from the University of Toledo, Ohio. He also holds a Bachelor of English and a Masters of Business Administration from the University of Texas at Brownsville. After graduation, he was employed at several corporations including Pixera, a digital multimedia processing company in Cupertino, CA, 3COM, a networking and communication company in Schaumburg, IL, and Mercantec, an E-Commerce company in Naperville, IL. He has more than 40 publications in the field, and has served as a reviewer/moderator for several scientific and educational journals and conferences. He joined UTB in the Spring of 2000. His areas of interest include Imaging, Visualization and Animation, Networking and Cyber Security, Web Design, Computer Graphics, and Linguistics.



Fig. 8 Original Lena image along with reduced gray levels images



Fig. 9 Reduced gray levels images obtained using Papamarkos Neural thresholding



Fig. 10 Reduced gray levels images obtained using standard K-means
Original Image



Fig. 11 Images obtained for 2-level thresholding (binarization) using the methods indicated



Fig. 12 Two-level quantization (binarization) of noisy Lena image images

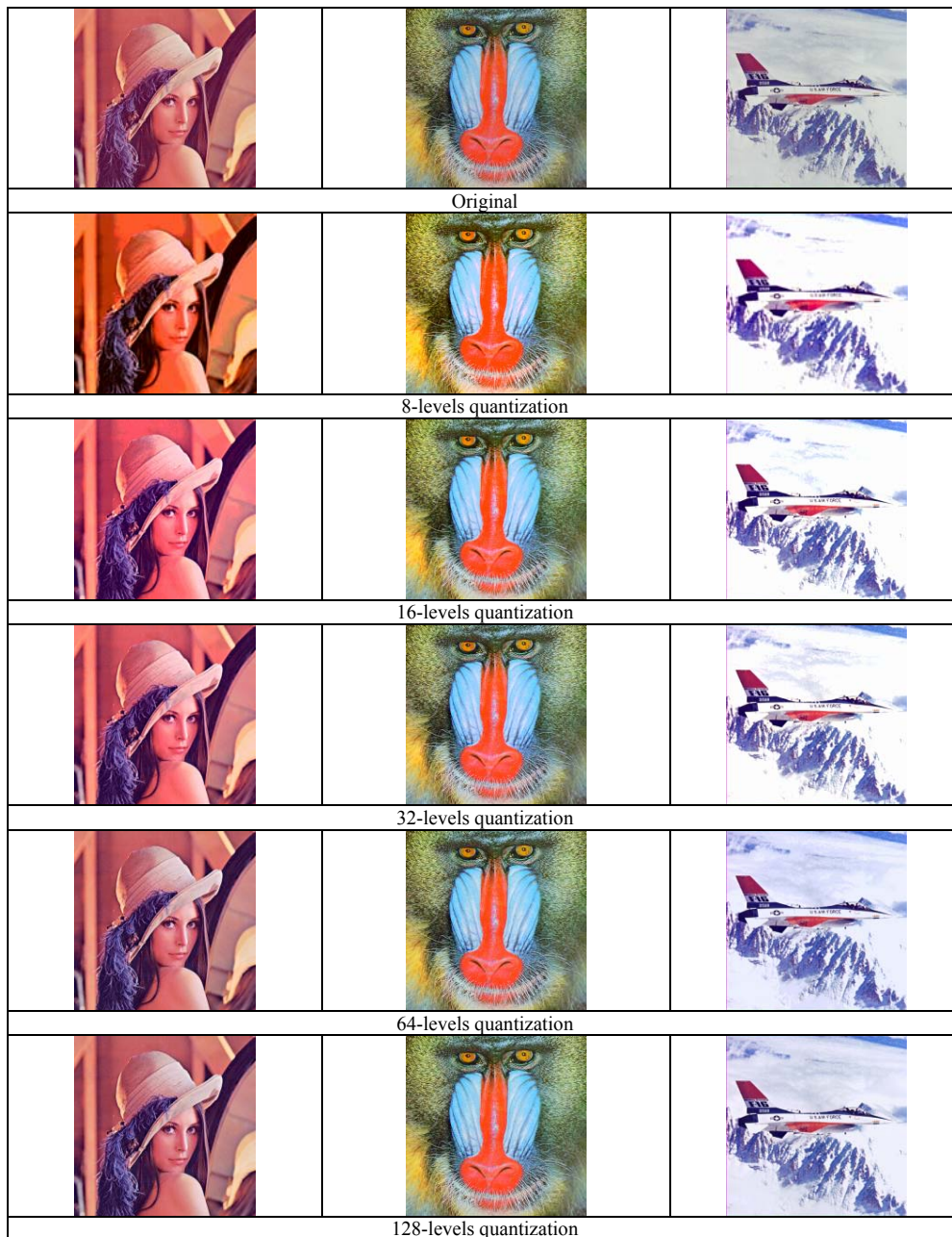


Fig. 13 Lena, Baboon, and F-16 results quantization results for the R, G, and B planes at the indicated levels of quantization

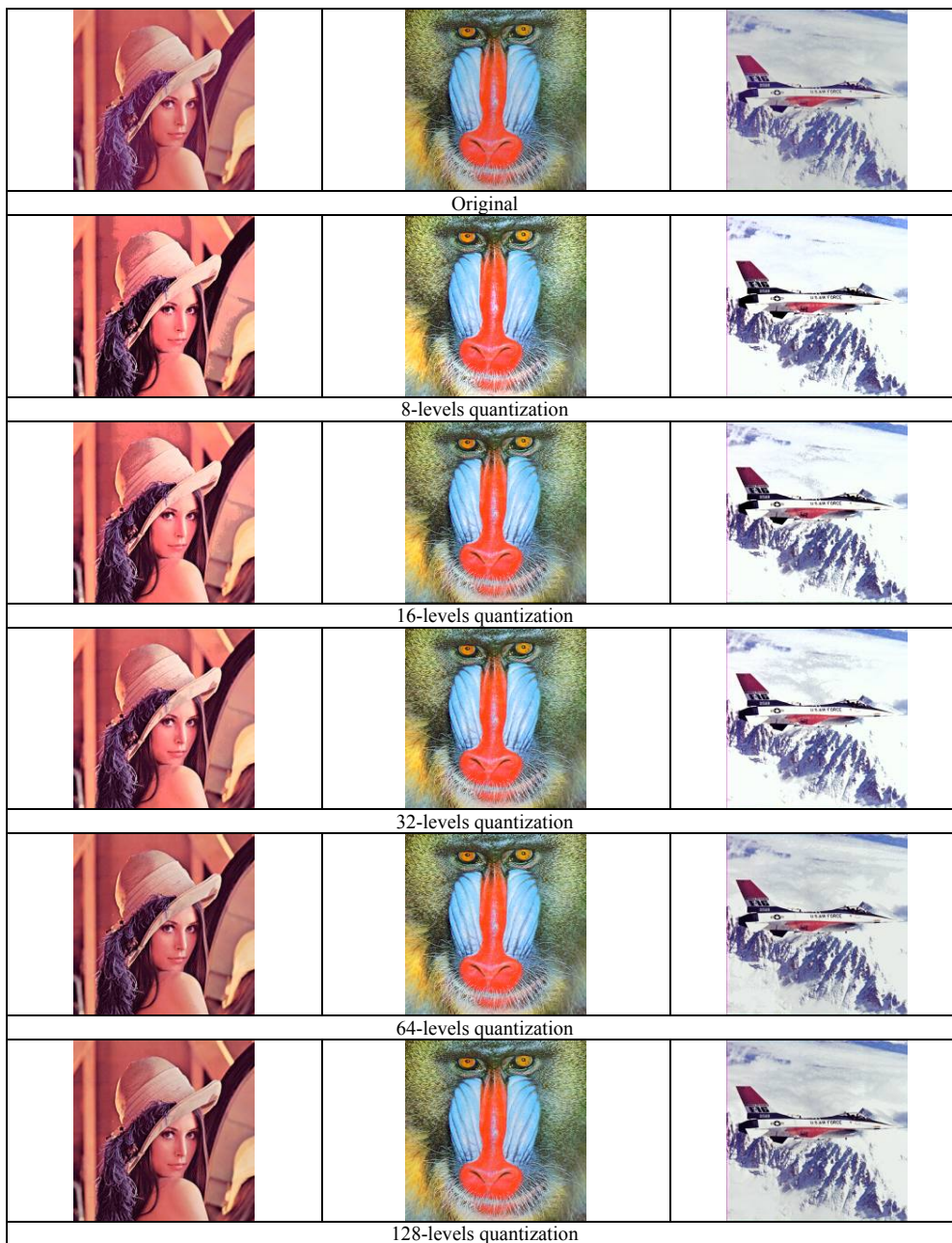


Fig. 14 Lena, Baboon, and F-16 results for the indicated number of levels for the V plane at the indicated levels of quantization